Dipole polarizabilities of medium-sized gold clusters

Jinlan Wang,[1,*] Mingli Yang,[2] Julius Jellinek,[3] and Guanghou Wang[4]
[1]*Department of Physics, Southeast University, Nanjing, 210096, People's Republic of China*
[2]*Department of Physics, Central Michigan University, Mount Pleasant, Michigan 48859, USA*
[3]*Chemistry Division, Argonne National Laboratory, Argonne, Illinois, 60439, USA*
[4]*National Laboratory of Solid State Microstructures, Nanjing University, Nanjing, 210093, People's Republic of China*
(Received 27 April 2006; published 16 August 2006)

The dipole polarizabilities of two families of low-lying structures, cage, and space filling, of the medium-sized Au_N (N=32,38,44,50,56) clusters are studied using gradient-corrected density functional theory and finite field method. Both dipole moments and polarizabilities exhibit clear shape-dependent features and the cage structures have systematically smaller dipole moments and larger polarizabilities than the space-filling isomers. The mean polarizability per atom increases with cluster size for the cage structures, but it decreases slowly and tends to approach a constant for the space-filling structures. A linearly correlation between polarizability and cluster volume is noted, complying with the jellium model prediction for spherical metal clusters. The electronic effects including HOMO-LUMO gap and ionization energy on polarizabilities are also explored. The geometric effects play a dominant role on the determination of the polarizability of the cluster over the electronic effects.

DOI: 10.1103/PhysRevA.74.023202 PACS number(s): 36.40.Vz, 73.22.−f

I. INTRODUCTION

Gold clusters and nanoparticles of finite size exhibit remarkable structural, physical, and chemical properties [1,2] and have been extensively investigated experimentally and theoretically over the past two decades [3–5]. Earlier studies indicated that small gold clusters favor planar structures and this planarity is attributed to relativistic effects [6–14]. Li *et al.* revealed that the Au_{20} cluster takes the tetrahedral pyramid structure that can be considered as a fragment of the face-centered cubic lattice [15]. The high stability of the Au_{20}-T_d structure was shown to arise from relativistic effect and aromaticity, which were not found for other coinage metal Ag and Cu clusters [16,17]. Later, Wei *et al.* found the pyramid bulk fragment structures for the Au_N clusters with N=15–23 and tubelike forms for N=24 and 26 [18,19]. For medium-sized gold clusters, truncated decahedral units were suggested for the sizes with diameters of 1–2 nm from x-ray powder diffraction [20,21]. Amorphous space-filling structures are energetically favored for Au_N of N=38,55,75, etc. from different level computations [22–25]. In contrast, recent studies have shown that hollow cages are good competitors for medium-sized gold clusters. A beautifully symmetrical icosahedra cage, referred as "golden fullerene," was predicted for Au_{32} computationally and its high stability is associated with aromaticity [26,27]. For Au_{42}, an icosahedral golden fullerene cage was also found as low energy structure [28]. We found that fullerene-based cages compete with space-filling structures for medium-sized Au_N at N=32,38,44,50,56 and the energetically preferred structure for Au_{50} is a cage with C_2 symmetry from relativistic density functional theory (DFT) computations [29]. The high stability of Au_{50} is associate with its aromaticity and big HOMO-LUMO gap.

Despite extensive studies of the geometric and electronic structures, there are very few studies on optical properties of intermediate-sized gold clusters [30–32]. Zhao *et al.* found the polarizability of two-dimensional Au_N, N=2–20 were strongly anisotropic at density functional theory level [30]. Wu *et al.* studied the second-order optical nonlinearity of the tetrahedral Au_{20} and found it possesses remarkable large molecular second-order optical nonlinearity resulting from charge transfer from edge atoms to vertex ones [31]. Wei *et al.* investigated the optical absorption spectra of Au_{32} and found that the icosahedra cage shows significant absorption peaks in the visible and near-uv range [32]. The goal of this paper is to study the dipole polarizabilities of the Au_N clusters of N=32,38,44,50,56, which are in two different structural growth patterns: hollow cages and space-filling structures. The size-dependent and shape-dependent dipole polarizabilities are investigated with the combination of gradient corrected density functional theory and finite field theory approach [33]. The geometric effect and the electronic effect on poliarizabilities are discussed. A close relationship between cluster volume and polarizability is observed and used to understand the shape dependence of polarizabilities.

II. COMPUTATIONAL METHODOLOGY

The equilibrium geometries were taken from our earlier work in which Perdew, Burke, and Ernzerhof (Ref. [34]) (PBE) parametrization of the exchange-correlation functional as well as a DFT-based relativistic semicore pseudopotential [35] (DSPP), and a double numerical basis set including d-polarization functions (DND) were used to identify the ground state structures. The choice of the functional and basis sets (PBE, DSPP, or DND) was based on extensive computations performed on the Au atom, and Au_N clusters of N=2–14 and 20 and the details can be found in Ref. [29]. All these structures were optimized without any symmetry

*Email address: jlwang@seu.edu.cn

 ©2006 The American Physical Society

TABLE I. The structures, relative energies (ΔE), HOMO-LUMO gaps (Δ), vertical ionization potentials (VIP), dipole moments, mean polarizability per atom ($\bar{\alpha}$) of the lowest energy cage and lowest energy space-filling conformations of Au_N, $N=32,38,44,50,56$.

System	Structure	ΔE (eV)	Δ (eV)	VIP (eV)	μ (Debye)	$\bar{\alpha}$ (Å^3/atom)
Au_{32}	Cage-I_h	0	1.527	6.835	0.000	4.814
	Space-filled-C_1	1.254	0.313	6.637	0.145	4.576
Au_{38}	Cage-D_6	0.385	0.110	6.313	0.000	5.060
	Space-filled-C_1	0	0.256	6.456	0.635	4.623
Au_{44}	Cage-D_2	0.067	0.173	6.654	0.000	5.193
	Space-filled-C_1	0	0.135	6.405	0.292	4.609
Au_{50}	Cage-D_{6d}	0	1.077	6.767	0.000	5.343
	Space-filled-C_1	0.434	0.230	6.503	1.098	4.594
Au_{56}	Cage-C_2	2.144	0.201	6.403	0.241	5.421
	Space-filled-C_1	0	0.310	6.643	0.824	4.564

constraint and were further confirmed to be true minima by vibrational frequency computations.

The finite field (FF) approach [33] implemented within the DMOL package [36] was used to calculate dipole moment and electric polarizability components at the PBE, DSPP, or DND level. The dipole moment μ_i and polarizability α_{ij} are defined respectively as

$$\mu_i = -\left(\frac{\partial E}{\partial F_i}\right) \tag{1}$$

and

$$\alpha_{ij} = -\left(\frac{\partial^2 E}{\partial F_i \partial F_j}\right) \quad (i,j=x,y,z), \tag{2}$$

where E is the total energy, F_i $(i=x,y,z)$ are components of the applied field in different directions. A numerical differential strategy is used in Kurtz's finite field method [33] to evaluate the dipole moment and polarizability. For each equilibrium structure, thirteen self-consistent field (SCF) computations are required with the field strengths of zero, $\pm F_i$, and $\pm 2F_i$ $(i=x,y,z)$. One of the problems in finite field method is the choice of field strength. The numerical accuracy against different field strengths has been assessed by Sim *et al.* [37] who suggested that stable linear and nonlinear polarizabilities can be obtained when F_i equals 0.001–0.005 a.u. In this work, the external field is applied along x, y, or z axis with F_i being set to 0.001 a.u. A tight SCF convergence criterion is adopted to ensure the precision of calculated polarizability. The mean polarizability per atom for the clusters, which is defined as

$$\bar{\alpha} = \frac{1}{3N}(\alpha_{xx} + \alpha_{yy} + \alpha_{zz}), \tag{3}$$

and the modulus of the dipole moments are discussed throughout this paper.

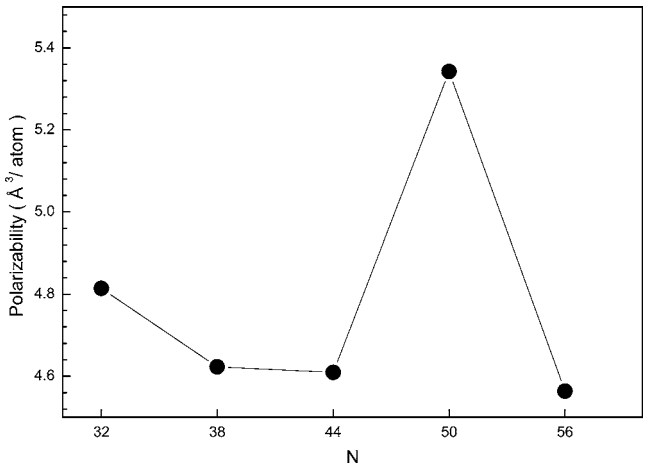

FIG. 1. Polarizability per atom of the lowest energy structures of Au_N, $N=32,38,44,50,56$.

III. RESULTS AND DISCUSSION

In our previous work, two types of energetically competitive structures, fullerene-based hollow cages and space-filling structures were obtained. Here, we focus on the shape and size dependence of the dipole moments and polarizabilities of these two different geometric conformations. It is note worthy to point out that a new cage structure with higher symmetry (D_{6d}) and larger HOMO-LUMO gap (1.077 eV) was found to have lower energy than the one reported in Ref. [29] by 0.256 eV for Au_{50} and was therefore used to explore the dipole polarizability in present study.

Table I presents the relative energies, the HOMO-LUMO gaps, the ionization potentials, the dipole moments, and the polarizabilities of the lowest energy cages and the space-filling structures of Au_N, $N=32,38,44,50,56$. The hollow cages have zero dipole moments except Au_{56}, while the space-filling structures have relatively large dipole moments. The differences in dipole moments mainly come from their different symmetries in geometry. The cage structures of Au_N, $N=32$, 38, 42, and 50, are highly symmetric (I_h, D_6, D_2, D_{6d}, respectively). Thus their charge distribute symmetrically around the geometric centers of the clusters and results in zero dipole moments. For Au_{56}, the cage has C_2 symmetry and smaller dipole moments (0.241 Debye) than the space-filling isomer (0.824 Debye). On the other hand, all the space-filling structures are nonsymmetric and inclined to have relatively big dipole moments. For the electric polarizability, the cages always give larger polarizabilities than the space-filling structures for all the sizes studied here. This indicates that the geometric effect has a significant influence on the polarizability of gold clusters.

Before we further explore the geometric effect on polarizability, let us first look into the size-dependent polarizability of the lowest energy structures of the Au clusters. As shown in Fig. 1, the polarizability of the cluster peaks at $N=32$ and 50, while the clusters at $N=38,44,56$ have much smaller values. This is own to the different geometrical features of the lowest energy structures of the Au clusters at different sizes. The lowest energy structures are hollow cages

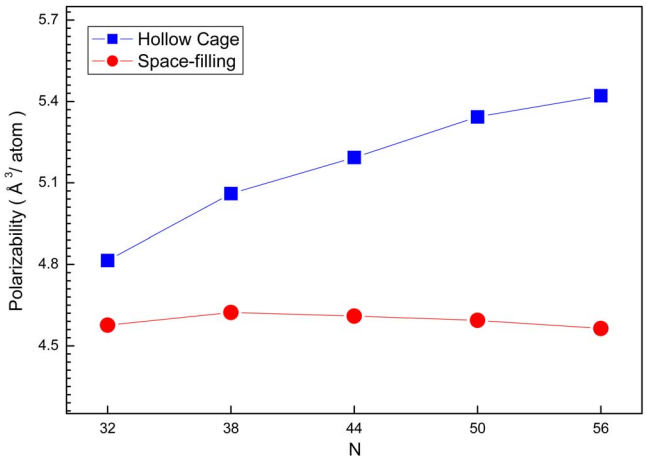

FIG. 2. (Color online) Polarizability per atom of the lowest energy cages and the lowest energy space-filling structures of Au_N, $N=32,38,44,50,56$.

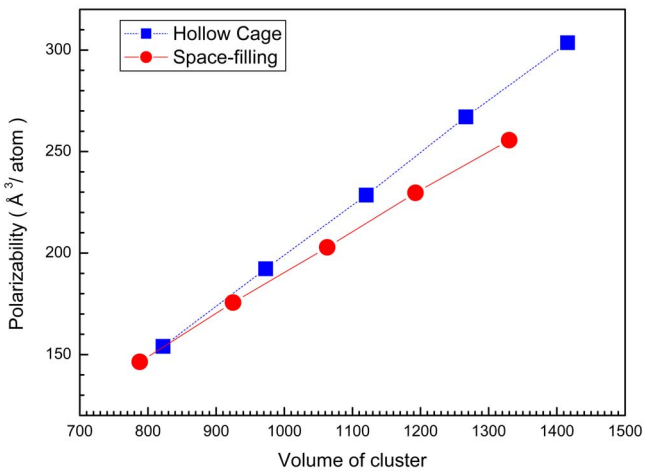

FIG. 3. (Color online) Total polarizability of the lowest energy cages and the lowest energy space-filling structures of Au_N, $N=32,38,44,50,56$ versus cluster volume.

for Au_{32} and Au_{50} but space-filling forms for $N=38$, 44, and 56. Moreover, the polarizabilities of $N=38,44,56$ are almost unaltered, indicating that the cage structure and the space-filling structure might have different polarizability behavior, that is, their polarizabilities are shape dependent.

To illustrate shape-dependent polarizability, we have investigate the polarizabilities of the hollow cage and the space-filling structures as a function of cluster size. As displayed in Fig. 2, the polarizabilities of the hollow cages are about 0.2–1.0 Å^3/atom larger than those of the space-filling structures. Moreover, the discrepancy between the two types of conformations increases with size. For Au_{32}, the polarizability of the cage structure is about 5% larger than that of the space-filling counterpart, while the difference increases to 18% for Au_{56}. More interestingly, the polarizability of the cage forms increases with size, while it decreases slowly and tends to approach a constant (around 4.6 Å^3/atom) for the space-filling conformations. This indicates that the polarizability of the space-filling structure is getting to saturate in this size range.

The shape-dependent polarizability can be further analyzed in terms of the volumes of electronic delocalization in the clusters. A close correlation between polarizability and cluster volume is displayed in Fig. 3, where the polarizabilities of both the cages and the space-filling structures increase linearly with their volumes, respectively. The cluster volume was computed by integrating all points in the space with electron density greater than 0.001 au, as recommended by Bader [38]. Therefore, what we have defined is electron delocalization volume rather than geometrical volume. The cage structure generally has larger volume than its space-filling isomer because there is less volume shared by multiple atoms in the latter. Polarizability measures the overall electronic charge redistribution in presence of an external field, usually favored by large volume of electron delocalization. The linear increase of polarizability with volume shown in Fig. 3 indicates that the volume is crucial in determining the polarizabilities of the gold clusters. Our findings comply with the classical polarizability of a conducting sphere [39], which is given rigorously in terms of the volume. In the jellium model, the polarizability of a spherical metal cluster can be expressed approximately as [39–41]

$$\alpha = (R + \delta)^3, \tag{4}$$

where R is the radius of the positive background charge and is the so-called spill-out parameter, simply interpreted as the distance the electronic density extends beyond the background positive charge. The right-hand term in Eq. (4) can be understood as the electron delocalization volume, what we defined above as cluster volume. Interestingly, both the cages and space-filling structures exhibit a linear dependence in polarizability, but in different patterns, indicating different electron delocalization or localization effects between them.

Our earlier study [29] has addressed that the space-filling structures are nonaromatic, while the cage structures are either aromatic or antiaromatic, implying different electron delocalization behaviors in these two kinds of configurations. To give a clear picture of the electron delocalization or localization, we plot the highest occupied molecular orbital (HOMO) of the cage structures and the space-filling structures of Au_N, $N=32,50$ in Fig. 4. It clearly shows that the electron densities of HOMO for these two cage structures are delocalized while their corresponding space-filling structures are localized. Such difference is also noted for clusters of $N=38$, 44, and 56, which are not presented here.

The electronic properties such as HOMO-LUMO gap and ionization energy usually have some influence on the polarizability of the cluster. For example, a simple perturbation theory suggested that polarizability should be inversely correlated to the HOMO-LUMO gap [42]. In this study, however, such correlation is not observed for the Au clusters. In contrast, we find that the cluster with bigger HOMO-LUMO gap tends to have larger polarizability at the same size. For Au_{32}, the HOMO-LUMO gap of the cage structure is 1.527 eV, much bigger than that of the space-filling isomer (0.313 eV), while its polarizability (4.817 Å^3/atom) is also larger than that of the space-filling isomer (4.576 Å^3/atom).

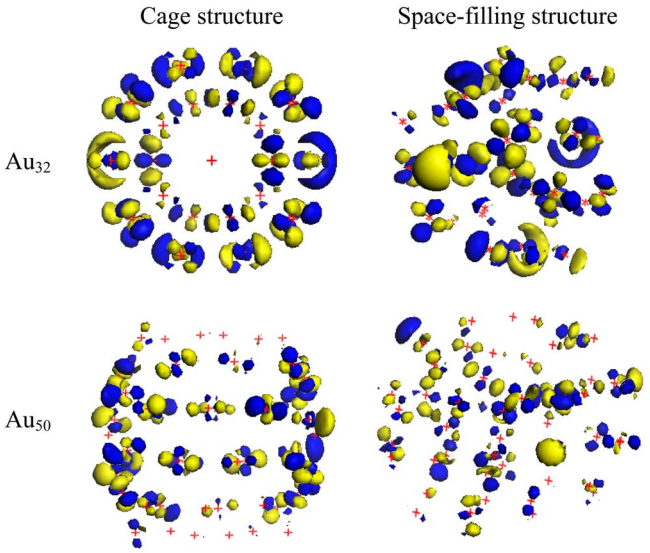

FIG. 4. (Color online) HOMO of the cage structures (left panels) and the space-filling structures (right panels) of Au_{32} and Au_{50}.

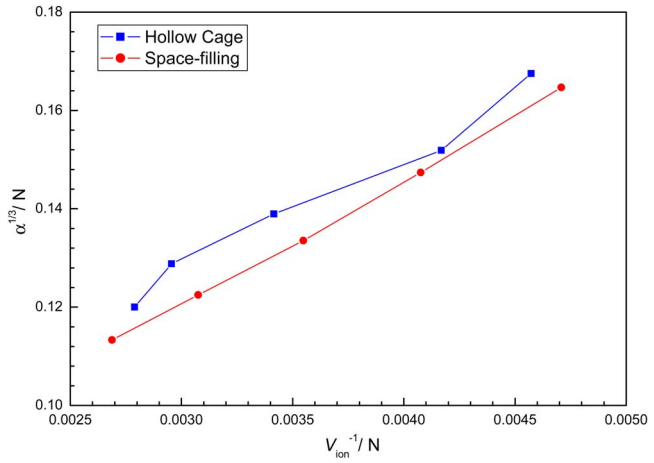

FIG. 5. (Color online) The relationship between the polarizability ($\alpha^{1/3}/N$) and the ionization potential ($V_{ion}{}^{-1}/N$) of the lowest energy cages and the space-filling structures for Au_N, $N=32,38,44,50,56$.

Similar results are observed for Au_{50} for which the HOMO-LUMO gap of the cage structure is 1.098 eV and the polarizability is 5.343 Å^3/atom, while the space-filling structure has the gap of 0.137 eV and the polarizability of 4.594 Å^3/atom, respectively. However, the cage structures of $N=38$, 44, and 56 have close HOMO-LUMO gaps with their space-filling isomers, but possess evidently larger polarizabilities. Similar results have also been reported for silicon and copper clusters [43] for which no simple correlation was observed between the polarizability and the HOMO-LUMO gap. In perturbation theory, polarizability is expressed as a sum of contributions from all excited states [44]. A clear correlation between polarizability and the HOMO-LUMO gap holds if the dominant excited state is mostly described by the transition from HOMO to LUMO. Our calculations reveal that the polarizabilities are only partially contributed from the HOMO to LUMO transitions, while the contributions from other transitions are not neglectable, making an unclear correlation between HOMO-LUMO gap and polarizability for these gold clusters.

The ionization energy is a quantity indicating the capability of the cluster to lose one valence electron. A recent study by Chandrakumar *et al.* [45] revealed that the cube root of polarizability per atom ($\alpha^{1/3}/N$) is inversely proportional to the ionization energy per atom ($V_{ion}{}^{-1}/N$) for both the sodium and lithium clusters of $N=2-10$. This is understandable since the higher ionization energy means a stronger binding of the valence electron to the cluster and the static polarizability is a measurement of the distortion of the electron density under an external static electric field. To explore the correlation between polarizability and ionization energy, the variation of $\alpha^{1/3}/N$ as a function of $V_{ion}{}^{-1}/N$ is displayed in Fig. 5 for both the cage and space-filling structures, respectively. First, the polarizability is clearly related to the IP if we discuss the values of cage and space-filling structures separately. $\alpha^{1/3}/N$ increases monotonically with $V_{ion}{}^{-1}/N$, the same as those revealed by Chandrakumar *et al.* for sodium and lithium clusters. Second, strong correlation is observed for the space-filling structures of which the $\alpha^{1/3}/N$ increasing linearly with $V_{ion}{}^{-1}/N$ for the space-filling structures, while no such simple linear dependence is observed for the cage structures. The deviation from the linear dependence for the cage structures is probably due to the shape variations among them. For the space-filling structures, their shapes do not change a lot from $N=32$ to 56, while the cage structures are spherical for $N=32$ and 50, but are ellipsoidal for $N=38$, 44, and 56. The different correlations between polarizability and ionization energy for the cages and the space-filling structures demonstrate again the geometric effect on the polarizability of the Au clusters.

IV. CONCLUSION

In summary, the dipole polarizabilities of the medium-sized gold clusters Au_N of $N=32$, 38, 44, 50, 56 have been studied within the framework of gradient-corrected density functional theory and finite field method. Two families of low-lying structures, hollow cage, and space filling, exhibit clear shape dependence in their dipole moments and polarizabilities. The cages possess smaller (zero) dipole moments and larger polarizabilities than the space-filling isomers. In the size range we studied, the mean polarizability per atom increases linearly with cluster size for the cage structures while it decreases slowly and tends to be a constant for the space-filling structures. Both the cage structures and the space-filling structures show linear dependence on the volume of the cluster but in different patterns, indicating a dominant role of electronic delocalization volume, which is closely related to the shape of the cluster, in determining the polarizabilities of Au clusters. The electronic effects including HOMO-LUMO gap and ionization energy to polarizability are also explored. No simple correlation is found between HOMO-LUMO gap and polarizability, while a shape-

dependent correlation is found between the ionization energy and the polarizability for the Au clusters.

ACKNOWLEDGMENTS

This work was supported by the Teaching and Researching Foundation for outstanding Young Faculty of Southeast University (JW) and by the Office of Basic Energy Sciences, Division of Chemical Sciences, Geosciences, and Biosciences, U.S. Department of Energy, Contract No. W-31-109-Eng-38 (J.J.). M.Y. thanks Professor K. A. Jackson for valuable discussion. J.W. thanks J. J. Zhao for providing the Au_{50}-D_{6d} cage structure and the computational resource (SGI Origin-2000 supercomputer) from Nanjing University.

[1] M. Haruta, T. Kobayashi, H. Sano, and N. Yamada, Chem. Lett. **2**, 405 (1987).
[2] G. C. Bond and D. T. Thompson, Gold Bull. **33**, 41 (2000).
[3] P. Schwerdtfeger, Angew. Chem., Int. Ed. **42**, 1892 (2003).
[4] P. Pyykkö, Angew. Chem., Int. Ed. **43**, 4412 (2004).
[5] M. C. Daniel and D. Astruc, Chem. Rev. (Washington, D.C.) **104**, 293 (2004).
[6] H. Hakkinen and U. Landman, Phys. Rev. B **62**, R2287 (2000).
[7] V. Bonacic-Koutecky, J. Burda, R. Mitric, M. F. Ge, G. Zampella, and P. Fantucci, J. Chem. Phys. **117**, 3120 (2002).
[8] J. L. Wang, G. H. Wang, and J. J. Zhao, Phys. Rev. B **66**, 035418 (2002).
[9] H. Hakkinen, M. Moseler, and U. Landman, Phys. Rev. Lett. **89**, 033401 (2002).
[10] E. M. Fernandez, J. M. Soler, I. L. Garzon, and L. C. Balbas, Phys. Rev. B **70**, 165403 (2004).
[11] L. Xiao and L. C. Wang, Chem. Phys. Lett. **392**, 452 (2004).
[12] F. Furche, R. Ahlrichs, P. Weis, C. Jacob, S. Gilb, T. Bierweiler, and M. M. Kappes, J. Chem. Phys. **117**, 6982 (2002).
[13] H. Hakkinen, B. Yoon, U. Landman, X. Li, H. J. Zhai, and L. S. Wang, J. Phys. Chem. A **107**, 6168 (2003).
[14] S. Gilb, P. Weis, F. Furche, R. Ahlrichs, and M. M. Kappes, J. Chem. Phys. **116**, 4094 (2002).
[15] J. Li, X. Li, H. J. Zhai, and L. S. Wang, Science **299**, 864 (2003).
[16] R. B. King, Z. Chen, and P. v. R. Schleyer, Inorg. Chem. **43**, 4564 (2004).
[17] J. L. Wang, G. H. Wang, and J. J. Zhao, Chem. Phys. Lett. **380**, 716 (2005).
[18] W. Fa, C. F. Luo, and J. M. Dong, Phys. Rev. B **72**, 205428 (2005).
[19] F. Wei and J. M. Dong, J. Chem. Phys. **124**, 114310 (2006).
[20] C. L. Cleveland, U. Landman, T. G. Schaaff, M. N. Shafigullin, P. W. Stephens, and R. L. Whetten, Phys. Rev. Lett. **79**, 1873 (1997).
[21] T. G. Schaaff, M. N. Shafigullin, J. T. Khoury, I. Verzmar, R. L. Whetten, W. G. Cullen, P. N. First, C. Gutierrez-Wing, J. Ascensio, and M. J. Jose-Yacaman, J. Phys. Chem. B **101**, 7885 (1997).
[22] I. L. Garzon, K. Michaelian, M. R. Beltran, A. Posada-Amarillas, P. Ordejon, E. Artacho, D. Sanchez-Portal, and J. M. Soler, Phys. Rev. Lett. **81**, 1600 (1998).
[23] K. Michaelian, N. Rendon, and I. L. Garzon, Phys. Rev. B **60**, 2000 (1999).
[24] J. P. K. Doye and D. J. Wales, New J. Chem. **22**, 733 (1998).
[25] T. X. Li, S. Y. Yin, Y. L. Ji, B. L. Wang, G. H. Wang, and J. J. Zhao, Phys. Lett. A **267**, 403 (2000).
[26] M. P. Johansson, D. Sundholm, and J. Vaara, Angew. Chem., Int. Ed. **43**, 2678 (2004).
[27] X. Gu, M. Ji, S. H. Wei, and X. G. Gong, Phys. Rev. B **70**, 205401 (2004).
[28] Y. Gao and X. C. Zeng, J. Am. Chem. Soc. **127**, 3698 (2005).
[29] J. L. Wang, J. Jellinek, J. J. Zhao, Z. F. Chen, R. B King, and P. von. S. Schleyer, J. Phys. Chem. A **109**, 9265 (2005).
[30] J. Zhao, J. Yang, and J. G. Hou, Phys. Rev. B **67**, 085404 (2006).
[31] K. C. Wu, J. Li, and C. S. Lin, Chem. Phys. Lett. **388**, 353 (2004).
[32] F. Wei, J. Zhou, C. F. Luo, and J. M. Dong, Phys. Rev. B **73**, 085405 (2006).
[33] H. A. Kurtz, J. J. P. Stewart, and K. M. Dieter, J. Comput. Chem. **11**, 82 (1990).
[34] J. P. Perdew, K. Burke, and M. Ernzerhof, Phys. Rev. Lett. **77**, 3865 (1996).
[35] D. R Hamann, M. Schluter, and C. Chiang, Phys. Rev. Lett. **43**, 1494 (1979).
[36] DMOL is a density functional theory (DFT) package distributed by Accelrys Inc. B. Delley, J. Chem. Phys. **92**, 508 (1990); **113**, 7756 (2000).
[37] F. Sim, S. Chin, M. Dupuis, and J. E. Rice, J. Phys. Chem. **97**, 1158 (1993).
[38] R. F. W. Bader, *Atoms in Molecules: A Quantum Theory* (Oxford University Press, New York, 1990).
[39] M. Brack, Rev. Mod. Phys. **65**, 677 (1993).
[40] D. R. Snider and R. S. Sorbello, Phys. Rev. B **28**, 5702 (1983).
[41] W. A. de Heer, Rev. Mod. Phys. **65**, 611 (1993).
[42] I. Vasiliev, S. Ogut, and J. R. Chelikowsky, Phys. Rev. Lett. **78**, 4805 (1997).
[43] K. A. Jackson, M. Yang, I. Chaudhuri, and Th. Frauenheim, Phys. Rev. A **71**, 033205 (2005).
[44] B. J. Orr and J. F. Ward, Mol. Phys. **20**, 513 (1971).
[45] K. R. S. Chandrakumar, T. K. Ghanty, and S. K. Ghosh, J. Phys. Chem. A **108**, 6661 (2004).